Determination of $CoSi_2$ Self-Aligned Nanostructures with Grazing Incidence X-ray Absorption Spectroscopy

Joshua D. Carter, Fang Shan, and Ting Guo*

Department of Chemistry, University of California, One Shields Avenue, Davis, California 95616

Received: November 10, 2004; In Final Form: December 24, 2004

Self-aligned nanostructures (SAN) made by reacting Co nanoparticles with crystalline Si substrates at high temperatures were studied with grazing incidence X-ray absorption spectroscopy (GI-XAS). The results from extended X-ray absorption fine structure (EXAFS) analysis and X-ray absorption near-edge spectroscopy (XANES) were used to identify SAN as crystalline $CoSi_2$. Theoretical calculations of EXAFS and XANES spectra of several crystalline cobalt silicides were performed with the FEFF8 package. On the basis of these studies, the SAN samples were determined to contain nearly pure $CoSi_2$.

Introduction

Characterization of the structure of nanomaterials has generally been performed with electron microscopy such as transmission electron microscopy (TEM) and electron diffraction (ED), especially when the materials can be isolated and are substrate-free.[1] For example, Au_{55} nanocrystals have been carefully scrutinized and their structure was determined by TEM.[2] If an adequate amount of nanomaterials can be obtained, and their aggregates can form ordered 3-D structures, X-ray diffraction (XRD) may be employed. As an example, the structure of Ga_{84} has been obtained by XRD.[3] However, when limited amounts of nanoscale materials coexist with a substantial amount of substrate materials, it is difficult to employ either ED or XRD to determine their structures.

We have recently shown that it is possible to use nanoparticles as fundamental building blocks to make quasi one-dimensional nanostructures, just as atoms or thin films have been used to make micro- and macrostructures in the past.[4] In that work, Co nanoparticles were deposited on and reacted with Si crystalline substrates at high temperatures. The products had unique nanostructures formed on the Si crystalline substrate. We term the new material self-aligned nanostructures (SAN). TEM studies revealed that those materials were crystalline, and it was speculated that SAN were made of $CoSi_2$ based on the conditions under which they were produced. Even though parts of the substrate could be thinned to sub-10-nm thickness via ion milling, it was still too thick to effectively use ED to determine the structure of SAN. As a result, most of the diffraction spots were from the Si substrate. Since Co and silicon could form several alloy epitaxial structures such as Co_2Si, CoSi, and $CoSi_2$ at different temperatures and they all have relatively small lattice mismatching with respect to crystalline Si,[5] it is difficult to conclusively identify the structures of SAN, and until now no direct evidence has been available. Because $CoSi_2$ is an excellent conductor that can be used as contacts, interconnects, and gates in future nanoelectronics and as field emission tips and IR detectors, it is important to verify whether the SAN are made of $CoSi_2$ or other Co−Si alloys.[6]

XAS is equivalently a local diffraction method and can be used to obtain detailed structural information.[7] More importantly, because different elements have absorption edges at different energies, XAS can eliminate most of the noise from the substrate. However, if the mass ratio of the sample to that of the substrate is too great, the elastically scattered X-rays can still dominate the fluorescent signals and deteriorate the signal-to-noise ratio to a level that no sensible results may be obtained.

To minimize the contribution of scattered X-rays from the substrate, we have employed grazing incidence X-ray absorption spectroscopy (GI-XAS), including extended X-ray absorption fine structure (EXAFS) analysis and X-ray absorption near-edge spectroscopy (XANES), to study the structure of SAN. GI-XAS has been used to examine various nanostructures in the past,[8−10] and it is well-suited for investigating samples at the surface. For example, at 0.17° angle of incidence, 8 keV X-rays are totally reflected by the Si wafer, which then allows only several nanometers or less penetration depth.

Co silicides have been investigated with XAS. Platow et al.[11,12] studied Co−Si thin films, and their results indicate that the XAS spectrum of $CoSi_2$ is very much different from that of CoSi, and the two structures have drastically different EXAFS patterns. In other studies, Rossi et al.[13] have investigated $CoSi_2$ thin films, and their analyses reveal that each Co has eight Si atoms in its nearest neighbors and 12 Co atoms in the second coordination shell. This is identical to that of the $CoSi_2$ bulk structure (CaF_2). Ersen et al.[14] theoretically studied the XANES and EXAFS of $CoSi_2$. It is found that $CoSi_2$ theoretical estimations are close to those measured experimentally.

In this work, we present both experimental and theoretical data that can be used to unambiguously demonstrate that SAN are crystalline $CoSi_2$. EXAFS and XANES results were obtained experimentally and simulated theoretically, and EXAFS data were fitted to obtain the structural parameters.

Experimental Section

Syntheses and Cleaning of SAN. Nanoparticles and SAN were prepared on the basis of our previous report.[4] In brief, Co nanoparticles were synthesized via the high-temperature thermodecomposition method.[15] Co nanoparticles (12 nm) were made and used to make SAN. Piranha solution [1:4 H_2O_2 (30%)/H_2SO_4 (concentrated)] cleaned Si (100) wafers (1 cm × 4 cm) were immersed in the nanoparticle solutions for a short time. The wafers were then retrieved and rinsed with deionized (DI) water and dried with Ar gas. All wafers were coated with nanoparticles in an identical manner, and approximately the

10.1021/jp044836q CCC: $30.25
Published on Web 02/05/2005

same amounts of nanoparticles were assumed to be deposited on those wafers. They were then set in a high-temperature furnace to react for a certain time, during which Ar (99.997%, Praxair) and H_2 (99.95%, Praxair) gases were fed through the furnace. Piranha solution was used to remove residual Co materials from the original SAN samples. Both original and cleaned SAN samples were studied with XAS.

The reacted wafers were inspected by scanning electron microscopy (SEM) (FEI XL-30 SFEG) and atomic force microscopy (AFM) (NanoScope III, Digital Instruments), and then used in GI-XAS measurements.

GI-XAS (Synchrotron Data Collection and Data Analysis). The GI-XAS measurements were performed on beamline 11-2 at Stanford Synchrotron Radiation Laboratory (SSRL). A double Si(220) crystal spectrometer was used to select and focus the synchrotron X-rays into a 200 μm $\times$ 200 μm beam. The bandwidth of the spectrometer was $\sim$1 eV. Routine procedures were used to optimize the positions of the samples so that the angle of incidence was about 0.17°, with the X-ray beam covering most of the 4 cm length of the SAN samples. A 29-channel Ge detector was used to detect the X-ray fluorescence from Co in the SAN. The detector was positioned at $\sim$20 cm away from the samples. Program SUPER was used to set up the detector, and program XAS was used to collect the EXAFS and XANES data.

Normally five sweeps were used for measuring a sample. All the channels in each sweep were summed and all sweeps were added for each measurement. EXAFSPAK and FEFF were used to process and fit the EXAFS data.[16]

Simulation with FEFF8 (EXAFS and XANES). FEFF8 package was used to simulate both XANES and EXAFS patterns of $CoSi_2$, CoSi, and Co_2Si.[17] Crystal structures in the literature were used for these calculations.[18] ATOMS was used to generate the coordinates for FEFF8, which was then used to calculate the XAS patterns. In EXAFS calculations, an ab initio self-consistent real space multiple scattering code was used to obtain the scattering potentials, the scattering phase shifts, the relativistic dipole matrix elements, and X-ray absorption cross section. The maximum scattering path length was set to be 11 Å. The Debye−Waller constants for Co−Si and Co−Co obtained from the experimental values in this study were used. In XANES simulations, full multiple scattering (FMS) calculations were used, which was implemented in FEFF8 through Green's function theory. The radius for FMS was set to 6 Å.

Results

The SAN were identified as crystalline materials from our previous study. Reactions were carried out at 900 °C, and reaction time was $\sim$10 s. After reactions, there were still non-SAN Co species left on the substrate. We then used Piranha solution to remove those Co species in those original SAN samples. Figure 1 shows the SEM images of SAN before (panel a) and after Piranha cleaning (panel b). Although it was not clear whether Piranha was effective to remove all the non-SAN Co forms, the results obtained in this report suggest that the Piranha-cleaned SAN samples contained almost exclusively $CoSi_2$.

Figure 2 shows the EXAFS data (panel a) and the Fourier transform (FT, phase-uncorrected; panel b) of the EXAFS of a Piranha-cleaned SAN sample made at 900 °C. A 2−10 $Å^{-1}$ k range of EXAFS data was used to obtain the FT. Two main peaks are observed at 2.3 and 3.5 Å (phase-corrected, see Table 1), similar to those found in $CoSi_2$ thin films.[19] Table 1 lists the fitted parameters and those simulated with FEFF and EXAFSPAK. The bulk $CoSi_2$ has eight first-shell neighbors and 12 second-shell neighbors with similar disorder for the two shells, and the fitted parameters were close to that of bulk $CoSi_2$.

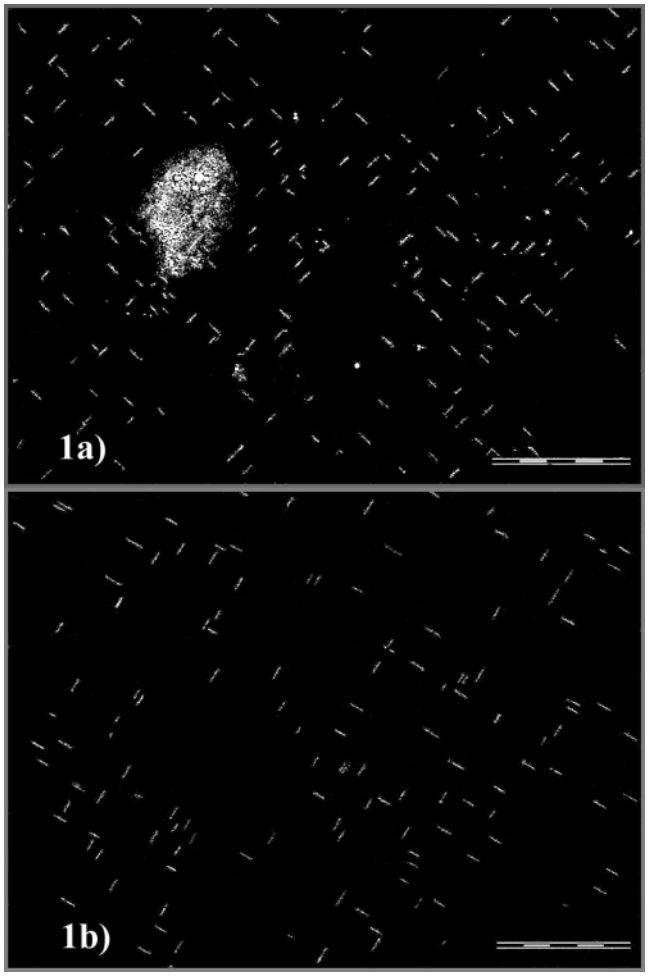

Figure 1. SEM images of SAN before (a) and after (b) Piranha cleaning. The scale bars are 2 μm.

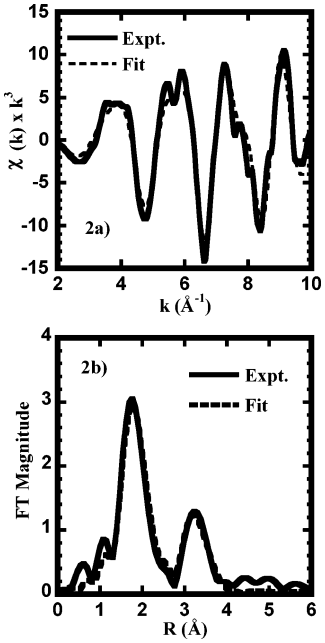

Figure 2. EXAFS data (a) and the Fourier transform (b) of EXAFS measurements (—) on a Piranha-cleaned SAN sample. Fitted plots are also shown (---). Fitted parameters are listed in Table 1.

TABLE 1: Fitted Parameters for the First and Second Coordination Shells of $CoSi_2$ SAN[a]

shell	S_0	R (Å)	N	σ^2 (Å^2)	ref
Co−Si	0.9	2.33	8.00	5.00×10^{-3}	this work
		2.32 ± 0.01	8	$(5.10 \pm 0.07) \times 10^{-3}$	Pong et al.[19]
Co−Co	0.9	3.84	12.00	9.19×10^{-3}	this work
		3.80 ± 0.02	12	$(8.14 \pm 0.03) \times 10^{-3}$	Pong et al.[19]

[a] Literature values for $CoSi_2$ bulk are also given.

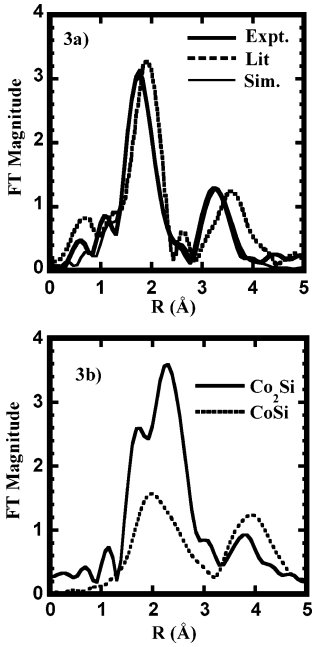

Figure 3. FT of EXAFS for $CoSi_2$ (a, thin solid line) and Co_2Si and CoSi (b) that were calculated with FEFF8 and then Fourier-transformed in EXAFSPAK. Also shown in panel a are the experimental data obtained in this work (thick solid line) and that by Pong et al. (dashed line).[19] Bulk crystalline structures were used for all three samples, and the Debye−Waller factors obtained from the fitted parameters and extrapolated on the basis of the additive principle were used.

The fitted parameters shown here represent the best fitting under physically allowed coordination numbers. Fitted parameters from other work are also listed in Table 1. The agreement between our results and those obtained on $CoSi_2$ thin films is evident.

We also simulated the EXAFS spectra of three crystalline Co−Si bulk materials, and Figure 3a shows the FT of simulated $CoSi_2$, the experimental data obtained in this work, and that measured by Pong et al.[19] Figure 3b shows the simulated EXAFS of CoSi and Co_2Si. As shown in Figure 3a, the simulated $CoSi_2$ spectrum matches well to the experimental FT profile of the SAN samples. In this simulation, multiple scattering paths were included and bulk $CoSi_2$ crystalline structure was used, as mentioned above. The single scattering Co−Si and Co−Co Debye−Waller factors σ^2 were 0.00500 and 0.00919, and the Debye−Waller factors for multiple scattering paths were adopted on the basis of the additive principle described in FEFF. We found that the contribution from those paths was small. Also shown in Figure 3a is the literature EXAFS profile (retrace) of $CoSi_2$ thin films measured by Pong et al. Although the FT of the EXAFS data from this thin film looked different from ours due to the ways in which those FT plots were processed, the fitted parameters were in good agreement, as shown in Table 1.

In contrast to $CoSi_2$, CoSi and Co_2Si had very different patterns: both have an extra peak at 2.3−2.6 Å (phase-corrected), which matched to those reported in the literature.[12]

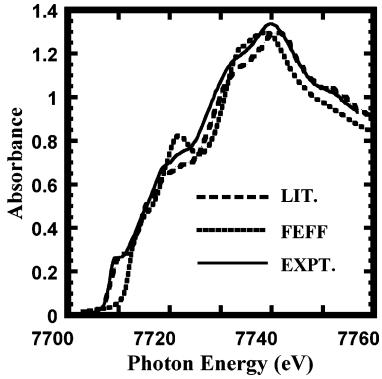

Figure 4. Measured, literature, and theoretical XANES spectra for $CoSi_2$. Both measured and simulated ones were calibrated (amplitude) to the literature profile.

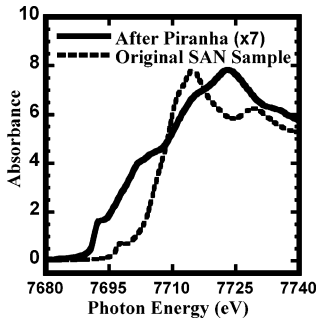

Figure 5. XANES for original and Piranha-cleaned SAN samples. The patterns and amplitudes are different for these two SAN samples, as shown.

This peak corresponds to Co−Co direct scattering as the nearest neighbors, indicating more Co atoms around the absorbing Co. This peak did not show up in any $CoSi_2$ samples because there are no Co−Co direct bonds. Both CoSi and $CoSi_2$ simulated patterns agree with other measured ones.

Figure 4 shows the measured XANES data (—) of Piranha-cleaned $CoSi_2$. An FEFF simulation is also shown in Figure 4. Also shown in Figure 4 is a retrace of the literature profile for $CoSi_2$ (− − −) obtained by Platow et al.[11] The XANES data obtained here were adjusted in absolute energy to match the absorption edge of the literature profile, and they follow the latter in every detail. The simulated XANES plot (···) in general agrees with the measured or the literature one, all of which have approximately four step increases before they reach the absorbance maxima. On the basis of these results, it is clear that SAN are $CoSi_2$. This result also shows that EXAFS and XANES should be intrinsically equivalent in terms of determining the structures. However, EXAFS is simpler to interpret while XANES data are easier to obtain.

We also measured the original SAN samples. Figure 5 shows that the Co XANES for the cleaned and original SAN. The signal intensity from the cleaned SAN sample is only 14% ($^1/_7$) that from the original sample. It is evident that the XANES pattern of the original SAN sample is different from those of the Piranha-cleaned SAN sample, as shown in Figure 5. On the basis of the XANES data, it is estimated that only approximately 10−20% of the Co reacted to form SAN, assuming that both samples contained the same amount of Co as deposited. From the XANES data, it is also clear that some Co was left unreacted with Si in the wafer after reactions at 900 °C, which was then oxidized when the samples were exposed to the air.

Discussion

The current GI-EXAFS measurements of SAN on Si wafer excluded the possibility of nanoparticle influence because the samples were cleaned with Piranha. Figure 5 shows the samples before and after the cleaning: the former shows a clear indication of oxidized Co nanoparticles on the wafer, and the latter was almost identical to the XANES profile of $CoSi_2$, suggesting that the sample was nearly pure $CoSi_2$.

Although SAN clearly fitted very closely with the parameters from $CoSi_2$ bulk and little resembled CoSi or Co_2Si, the parameter space in our fitting process was explored. Three scenarios were considered. In the first one, the coordination numbers for the first and second coordination shells were fixed at 8 and 12 and other parameters were optimized. In the second, we optimized all the parameters including the coordination numbers of the two coordination shells. In this case, the goodness of the fitting was marginally improved. However, higher shells had to be included. In the third case, the coordination number for Co−Co was optimized while disorders and Co−Si coordination number for the bulk were used. The coordination number for Co−Co was found to be 5−10% below that of the bulk.

The fitted parameters for the first scenario, as shown in Table 1, corresponded to the bulklike coordinate numbers for the first and second shells and the disorder for Co−Si, except that the disorder for the Co−Co (second shell) was slightly bigger, by 10−15%. This was expected due to the fact that $CoSi_2$ has small lattice mismatching (1%) compared with the Si substrate.[20] The results from the second scenario were less satisfactory because less confined parameter space led to multiple mathematically equally good fits that were difficult to explain physically. On the other hand, under the third scenario the goodness of fitting was almost identical (worse by 2%) to the first fitting scenario. This scenario was equally plausible as the first one. In this case, the lower coordination number for Co−Co could be caused by the smaller dimensions of $CoSi_2$ SAN. Assuming rectangular shapes for SAN, the slightly reduced coordination number for Co−Co could be explained by the size of the SAN of the order of 3 nm × 20 nm × 100 nm. Because there were still Si atoms around the five facets of the rectangular SAN, the reduction to Co−Si coordination numbers was much less. Further GI-EXAFS experiments with larger k ranges are needed to conclusively differentiate the validity of these three scenarios.

It is possible to use the three simulated forms of Co−Si to determine the relative weight of each composition in the Piranha-cleaned sample. A simple estimation, using the peaks at 2.6 and 3.5 Å, reveals that the SAN sample contained >97% $CoSi_2$.

The calculated XANES pattern for $CoSi_2$ was also shifted in energy to match that of the literature value. We performed similar calculations on CoO and compared its absorption edge to the literature value of the absorption edges, and we found a similar shift (−3 eV) was needed to match the theoretical XANES pattern to the literature one.

It is worth pointing out that a pure form of material should be employed in the XANES/EXAFS studies. In our case, it means that the amount of Co nanoparticles partaking in the high-temperature reactions should be limited to make sure that all Co reacted to form SAN if Piranha cleaning was not effective. It also indicates that GI-XAS with synchrotron sources can now provide data of adequate S/N ratios for measuring even monolayers of samples or for monitoring reactions between a submonolayer of nanoparticles and the crystalline substrate.

This work has also clearly demonstrated that GI-XAS can be used to study small amounts of nanostructures on thick substrates. On the basis of the dimensions and density of SAN in the Piranha-cleaned sample, one can estimate the amount of Co in the 4 cm × 200 μm stripe to be a few to a few tens of nanograms. Such small amounts are difficult to study by bulk XRD. Although ED can be used to investigate individual SAN, the sample has to be prepared so that there is almost no Si substrate around the SAN; otherwise diffraction patterns from Si would obscure that from $CoSi_2$. Therefore, GI-XAS is a generally good method to study nanostructures on surfaces or at interfaces.

Conclusion

Self-aligned nanostructures (SAN) made by reacting Co nanoparticles with crystalline Si substrates at high temperatures were studied with grazing incidence X-ray absorption spectroscopy (GI-XAS). These SAN were identified as crystalline $CoSi_2$ on the basis of results from extended X-ray absorption spectroscopy (EXAFS) analysis and X-ray absorption near-edge spectroscopy (XANES). The Co−Si shell closely resembles the bulk with similar coordination number, bond distance, and disorder. The Co−Co second shell can be fitted with either a slightly smaller coordination number or slightly larger disorder than those of the bulk. These different values can be attributed to either the reduced dimensions of $CoSi_2$ SAN or the lattice-mismatch-induced disorder in SAN or both. Theoretical calculations of EXAFS and XANES spectra of crystalline Co_2Si and CoSi counterparts with the FEFF8 package were carried out to demonstrate that the SAN investigated here was nearly pure $CoSi_2$. It is estimated that Piranha-cleaned SAN samples contain almost exclusively $CoSi_2$ crystalline nanostructures.

Acknowledgment. This work is partially supported by an NSF Career Award (CHE0135132) and the Camille and Henry Dreyfus Foundation. Acknowledgment is made to the donors of the Petroleum Research Fund, administrated by the American Chemical Society, for partial support of this research. We thank the excellent staff at Stanford Synchrotron Radiation Laboratory (SSRL) for experimental support. We are grateful to DOE for support of the facility.

References and Notes

(1) Wang, Z. L. *Characterization of nanophase materials*; Wiley−VCH: Weinheim, Germany, and New York, 2000.

(2) Schmid, G.; Pugin, R.; Sawitowski, T.; Simon, U.; Marler, B. *Chem. Commun.* **1999**, 1303−1304.

(3) Schnepf, A.; Schnockel, H. *Angew. Chem., Int. Ed.* **2001**, *40*, 712−715.

(4) Carter, J. D.; Cheng, G.; Guo, T. *J. Phys. Chem. B* **2004**, *108*, 6901−6904.

(5) Pearson, W. B. *A handbook of lattice spacings and structures of metals and alloys*; Pergamon Press: New York, 1967.

(6) *Silicide Thin Films—Fabrication, Properties, and Applications*; Tung, R., Maex, K., Pellegrini, P. W., Allen, L. H., Eds.; MRS: Boston, MA, 1996; Vol. 402.

(7) Koningsberger, R. D. C. A. *X-ray Absorption: Principles, Applications, Techniques of EXAFS, SEXAFS and XANES*; John Wiley & Sons: New York, 1988.

(8) Bargar, J. R.; Trainor, T. P.; Fitts, J. P.; Chambers, S. A.; Brown, G. E. *Langmuir* **2004**, *20*, 1667−1673.

(9) Towle, S. N.; Bargar, J. R.; Brown, G. E.; Parks, G. A. *J. Colloid Interface Sci.* **1999**, *217*, 312−321.

(10) Fitts, J. P.; Trainor, T. P.; Grolimund, D.; Bargar, J. R.; Parks, G. A.; Brown, G. E. *J. Synchrotron Radiat.* **1999**, *6*, 627−629.

(11) Platow, W.; Wood, D. E.; Burnette, J. E.; Nemanich, R. J.; Sayers, D. E. *J. Synchrotron Radiat.* **2001**, *8*, 475−477.

(12) Platow, W.; Wood, D. K.; Tracy, K. M.; Burnette, J. E.; Nemanich, R. J.; Sayers, D. E. *Phys. Rev. B* **2001**, *6311*, 5312−+.

(13) Rossi, G.; Jin, X.; Santaniello, A.; DePadova, P.; Chandesris, D. *Phys. Rev. Lett.* **1989**, *62*, 191−194.

(14) Ersen, O.; Pierron-Bohnes, V.; Tuilier, M. H.; Pirri, C.; Khouchaf, L.; Gailhanou, M. *Phys. Rev. B* **2003**, *6709*, 4116.
(15) Puntes, V. F.; Krishnan, K. M.; Alivisatos, A. P. *Science* **2001**, *291*, 2115−2117.
(16) http://www-ssrl.slac.stanford.edu/exafspak.html.
(17) http://leonardo.phys.washington.edu/feff/.
(18) Geller, S. *Acta Crystallogr.* **1955**, *8*, 83−87.
(19) Pong, W. F.; Chang, Y. K.; Mayanovic, R. A.; Ho, G. H.; Lin, H. J.; Ko, S. H.; Tseng, P. K.; Chen, C. T.; Hiraya, A.; Watanabe, M. *Phys. Rev. B−Condens. Matter* **1996**, *53*, 16510−16515.
(20) Alberti, A.; La Via, F.; Spinella, C.; Rimini, E. *Microelectron. Eng.* **2001**, *55*, 163−169.